

## Probing magnetic singularities during magnetization process in FePd films

Aurélien Masseboeuf,<sup>a)</sup> Thomas Jourdan,<sup>b)</sup> Frédéric Lançon, Pascale Bayle-Guillemaud, and Alain Marty

INAC, CEA, SP2M, F-38054 Grenoble, France

(Received 6 August 2009; accepted 29 October 2009; published online 24 November 2009)

We report the use of Lorentz microscopy to observe the domain wall structure during the magnetization process in iron-palladium thin foils. We have focused on the magnetic structure of domain walls of bubble-shaped magnetic domains near saturation. Regions are found along the domain walls where the magnetization abruptly reverses. Multiresolution magnetic simulations showed that these regions are vertical Bloch lines (VBL) and that the different bubble shapes observed are related to the inner structure of the VBL. Combining these two complementary methods, we were thus able to probe the presence of magnetic singularities as small as Bloch points in the inner magnetization of the domain walls. © 2009 American Institute of Physics.

[doi:10.1063/1.3266825]

It has been shown that alloys with perpendicular magnetic anisotropy (PMA) are good candidates for applications in future recording media with high density storage capacity or in magnetological devices.<sup>1</sup> Recently such materials, namely, iron-palladium (FePd) alloys have been used in spin-valves where they act as the polarizer and the free layer.<sup>2</sup> These devices are believed to work through the nucleation of a reversed domain followed by the propagation of a domain wall.<sup>3</sup> Understanding the properties and the structure of domain walls in FePd materials is therefore of primary importance. The magnetic configuration of FePd alloys has been extensively investigated by means of magnetic force microscopy imaging,<sup>4,5</sup> x-ray scattering,<sup>6</sup> and numerical simulations.<sup>7</sup> Moreover it has been shown recently that it is possible, using Lorentz transmission electron microscopy (LTEM), to image the magnetic distribution in PMA material thin foils at the domain wall scale,<sup>8</sup> below 10 nm. In addition, a magnetic field can be applied to perform magnetization process. Here we show that it is possible to probe the magnetic configuration inside the domain wall over dimensions smaller than the expected spatial resolution.

Along a domain wall one can find some regions, known as Bloch lines, where the sense of the magnetization abruptly reverses. In PMA materials, where domain walls are Bloch-type walls, Bloch lines perpendicular to the domain wall orientation can be expected. These lines are called vertical Bloch lines (VBL). VBL were extensively studied in the 80 s in garnets, both experimentally<sup>9–11</sup> and numerically.<sup>12–15</sup> Observations were possible using magneto-optical microscopy due to the large width of domain walls in garnets ( $\delta \approx 0.1 \mu\text{m}$ ). This large value has to be compared with the domain wall width in FePd of around 8 nm,<sup>16</sup> well below the resolution of optical methods. The simulation of the magnetic structure in garnets is also much easier than for FePd. Indeed, in garnets the very high quality factor  $Q = 2K/(\mu_0 M_s^2) \approx 8$ , where  $K$  is the anisotropy constant and  $M_s$  the saturation magnetization, ensures that the Bloch line

width is far larger than the domain wall width. It is thus possible to use a local approximation for the demagnetizing field;<sup>13</sup> the field depends only on the component of the magnetization perpendicular to the wall. This assumption is *a priori* not valid in the case of FePd, which exhibits smaller values of  $Q$  in the order of 1.6.

The aim of this letter is to show that an original magnetic simulation coupled to recent developments in LTEM permits to deduce the magnetic structure of such small magnetic defects as VBL in domain walls of FePd thin films. We focus in this work on VBL which are trapped in magnetic bubbles appearing near the saturation state.

A thin layer of L1<sub>0</sub>-FePd (37 nm) has been deposited on a “soft” layer of chemically disordered FePd<sub>2</sub> layer, grown on a MgO (001) substrate by molecular beam epitaxy.<sup>17</sup> The soft layer is used to enhance the recording efficiency in perpendicular recording hard drives (see for example section 2.4 of Ref. 18). The sample for LTEM has been then prepared by mechanical polishing and ion milling. The microscope used is a JEOL 3010 fitted in with a Gatan imaging filter for contrast enhancement by zero-loss filtering.<sup>19</sup> The *in situ* magnetization is performed with the objective lens while imaging is realized with the objective mini lens traditionally used for low magnification imaging. The field produced by the objective lens has been carefully calibrated by inserting a dedicated sample holder mounted with a Hall probe before the experiment.

We measured the half hysteresis loop of the film in Fresnel mode.<sup>20</sup> The complete description of this magnetization process can be found elsewhere.<sup>8</sup> For a field of 775 mT, just before the complete saturation of the magnetic layer, a focal series has been performed. Figure 1 shows the focal series reconstruction using the transport-of-intensity equation<sup>21</sup> (TIE). The magnetic information is originally mixed with an electrostatic contribution<sup>22</sup> which has been removed by considering a constant variation of the thickness of the sample.<sup>16</sup> Due to the Lorentz force and the transmitted electrons collection, LTEM is sensitive to the magnetic induction integrated along the electron beam direction in the TEM. Formally, the information probed is not directly related to the magnetization of the sample but to the magnetic induction. However, assuming that stray fields on both sides

<sup>a)</sup>Present Address: CNRS, CEMES, F-31055 Toulouse Cedex, France. Electronic mail: aurelien.masseboeuf@cemes.fr.

<sup>b)</sup>Present Address: CEA, DEN, Service de Recherches de Métallurgie Physique, F-91191 Gif-sur-Yvette, France.

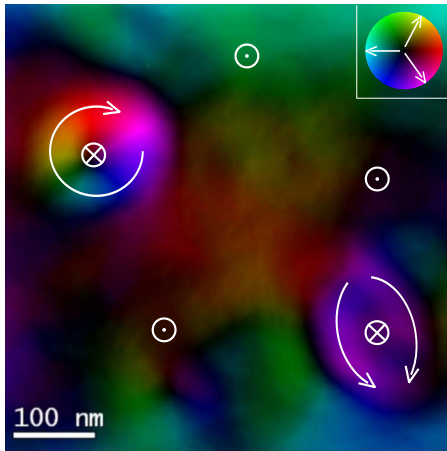


FIG. 1. (Color online) Magnetic induction mapping of the FePd thin film at 775 mT using TIE solving (3 images used for the reconstruction). The color scale used here is explained by the color wheel. Arrows are also used to emphasize the magnetic induction. Perpendicular induction (i.e., magnetization inside the domains) is deduced from the whole magnetization process (saturation state should be up).

of the layer are antiparallel, the integrated induction may be considered approximately the same as the integrated magnetization.

In Fig. 1 we can clearly see two types of magnetic bubbles. On the upper left corner one can see a magnetic bubble where the magnetization swirls continuously along the domain wall between the residual magnetic domain (indicated as down in Fig. 1) and the reversed domain. On the bottom right corner, one finds a magnetic bubble where the magnetization experiences two rotations of  $180^\circ$  resulting in two “different” domain walls pointing in similar directions.

At this point of the hysteresis loop a lot of bubbles are present in the film and both kinds of bubbles can be easily found. The two switching points observed in the second bubble type are supposed to be VBL.<sup>23</sup> It must be noticed that the geometric deformation observed for the bubble with two VBL (the bubble exhibiting a *lemon* shape) is fully reproducible.

In order to investigate the internal structure of these lines and the role of the lines on the shape of the bubbles, we have performed magnetic simulations on bubbles with and without VBL. Due to the large range of scale needed to model these objects, we have developed and used a multiresolution method. This method uses a varying mesh size technique to achieve both computational efficiency and numerical accuracy (details on the method can be found in Ref. 24). This is particularly useful in that case of magnetic bubbles as the inner and outer part of the bubble can be loosely meshed while the domain wall and the VBL need to be densely meshed.<sup>25</sup> Moreover, the code we used has the particularity to take into account the atomic structure of the material which is ignored in standard micromagnetic codes. The size of the micromagnetic mesh is automatically adapted and the system can be described at the atomic scale for high spatial variations of magnetization. We used this mixed micromagnetic/atomic level mode to check that Bloch point (BP) can be correctly simulated with a micromagnetic approach.<sup>26</sup> Then the sole multiscale micromagnetic mode was used to perform the calculations on bubbles. The decrease in the number of mesh cells is evaluated to around a factor of 8 compared to a single level micromagnetic code.

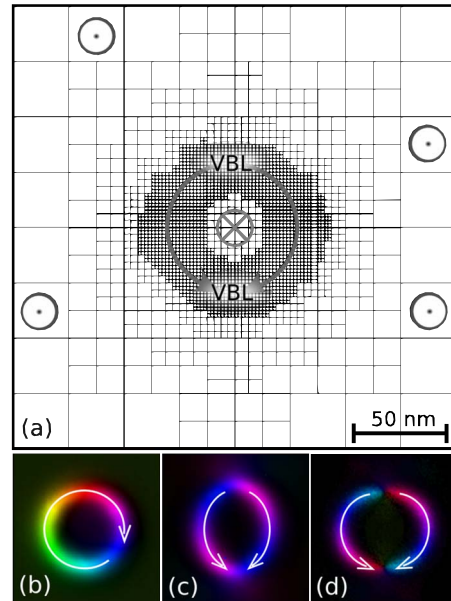


FIG. 2. (Color online) (a) Mesh distribution obtained for a typical magnetic bubble in our system (corresponding to the middle plane of the foil). The direction of magnetization as well as the position of the VBL have been added for clarity. (b–d) Magnetic multiresolution simulations of three different magnetic bubbles (lateral size of the view:  $90 \times 90$  nm, whole system:  $218 \times 218$  nm). The magnetization has been integrated along the observation direction to correspond to LTEM measurements. (b) A magnetic bubble with no VBL. (c) A magnetic bubble with two VBL, both VBL contain no Bloch point (BP). (d) A magnetic bubble with two VBL, each VBL contains a BP.

As an example a mesh distribution obtained for our system is given in Fig. 2(a).

In these simulations the saturation magnetization is  $M_s = 10^6$  A m<sup>-1</sup>, the anisotropy constant is  $K = 10^6$  J m<sup>-3</sup>, and the exchange stiffness constant<sup>27</sup> is  $A = 7 \times 10^{-12}$  J m<sup>-1</sup>. With these parameters the exchange length is  $\Lambda = \sqrt{2A/(\mu_0 M_s^2)} = 3.3$  nm. Two different thicknesses have been considered as follows: 15 and 20.7 nm. In Figs. 2(b)–2(d) the integrated magnetization along the thickness obtained from the simulations is shown for a bubble without VBL (b) and two bubbles with VBL for thicknesses of 15 (c) and 20.7 nm (d) in a field of 0.25 and 0.3 T, respectively. It can be seen that for a thickness of 15 nm [Fig. 2(c)] the bubble is deformed in agreement with the LTEM observations, whereas for a thickness of 20.7 nm its shape remains circular [Fig. 2(d)].

The modification of the shape can be explained by analyzing precisely the structure of the VBL for the two thicknesses envisaged. Two kinds of VBL can thus be found. In the case of a small thickness, the magnetization is uniform along the VBL [Fig. 3(a)], whereas it reverses along the VBL in the second case (large thickness), which leads to a magnetic singularity called a BP [Fig. 3(b)]. The reason for the transition is a competition between the exchange and demagnetizing energies; the presence of a BP leads to an increase in the exchange energy, whereas the demagnetizing energy decreases because the magnetization in the two segments of the line is aligned along the stray field generated by the domains.

Such a transition as a function of the thickness  $h$  has been reported by Hubert to be  $h = 7.3 \Lambda$  with an analytical model for a straight domain wall.<sup>28</sup> According to our simulations for the particular geometry considered here, the transition is found between 4.5 and 6.3  $\Lambda$ . Given the thickness

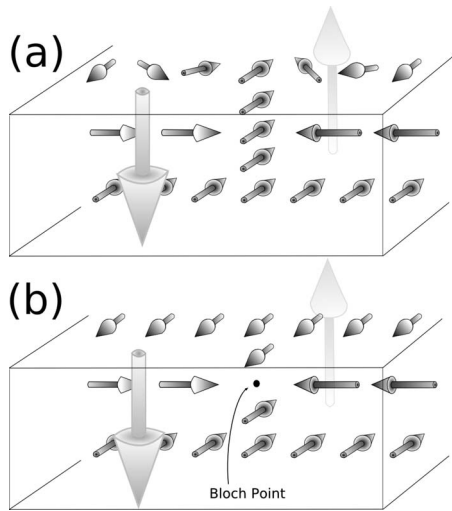


FIG. 3. (a) Vertical Bloch line (VBL) without a Bloch point (BP). The upper Néel cap of the Bloch wall is experiencing a swirl of 360°. (b) VBL with a BP. The Néel caps on each surface remain antiparallel.

$h=11.2 \text{ \AA}$  of the films observed by LTEM, the VBL should contain a BP, which is not consistent with the deformed states observed. However, the soft layer under the  $L1_0$  FePd film changes the magnetic configuration and alters the respective contributions of the exchange and demagnetizing terms to the energy. As described in a previous article,<sup>29</sup> the main role of the soft layer on the domain wall is an enhancement of the size (and as a consequence, the thickness) of the bottom Néel cap of the Bloch walls. This vertical asymmetry could thus favor the configuration with no BP by increasing the dipolar energy.

The deformation observed in the absence of BP gives rise to a reduction in magnetic charges;<sup>25</sup> it is analogous to the small buckling of the magnetization identified in straight domain walls in garnets.<sup>15</sup> In these materials, the buckling reduces the so-called “dipolar”  $\pi$  charges which are related to the variation of the magnetization perpendicular to the domain wall. In the case of FePd, the lower quality factor  $Q$  reduces the lateral extension of the VBL, which leads to large “monopolar”  $\sigma$  charges. A far larger buckling than could be expected following the studies on garnets is obtained: beside a reduction in  $\pi$  charges, it also reduces  $\sigma$  charges by a compensation of these two types of charges. It is worthy to note that the magnetization is oriented in the same direction in both VBL, so that the 360°-like domain walls are located on opposite surfaces. To compensate  $\sigma$  and  $\pi$  charges, a different orientation in the VBL would lead to a “heart”-shape bubble, which is not found to be stable in our simulations.

To conclude, in this letter we have highlighted the very high resolution obtained by combining LTEM and multiresolution simulations. The resolution we achieved by conven-

tional electron microscopy enables us to probe magnetic singularities well below the LTEM spatial resolution. Furthermore a main advantage of the varying mesh size code was its rapidity and its low memory requirements. In that case the number of cells was reduced by a factor of around 8 with respect to a standard finite difference micromagnetic code. The comparison between the two methods has shown that it is possible to determine the inner magnetic configuration of a VBL, namely, the presence or the absence of a BP in its structure.

- <sup>1</sup>D. Weller, A. Moser, L. Folks, M. E. Best, W. Lee, M. F. Toney, M. Schwickert, J.-U. Thiele, and M. F. Doerner, *IEEE Trans. Magn.* **36**, 10 (2000).
- <sup>2</sup>T. Seki, S. Mitani, K. Yakushiji, and K. Takanashi, *Appl. Phys. Lett.* **88**, 172504 (2006).
- <sup>3</sup>T. Seki, S. Mitani, and K. Takanashi, *Phys. Rev. B* **77**, 214414 (2008).
- <sup>4</sup>A. Asenjo, J. Garcia, D. Garcia, A. Hernando, M. Vazquez, P. Caro, D. Ravelosona, A. Cebollada, and F. Briones, *J. Magn. Magn. Mater.* **196**, 23 (1999).
- <sup>5</sup>Y. Samson, A. Marty, R. Hoffmann, V. Gehanno, and B. Gilles, *J. Appl. Phys.* **85**, 4604 (1999).
- <sup>6</sup>M. Mulazzi, K. Chesnel, A. Marty, G. Asti, M. Ghidini, M. Solzi, M. Belakhovsky, N. Jaouen, J. M. Tonnerre, and F. Sirotti, *J. Magn. Magn. Mater.* **272**, E895 (2004).
- <sup>7</sup>J. C. Toussaint, A. Marty, N. Vukadinovic, J. B. Youssef, and M. Labrune, *Comput. Mater. Sci.* **24**, 175 (2002).
- <sup>8</sup>A. Masseboeuf, C. Gatel, A. Marty, J. C. Toussaint, and P. Bayle-Guillemaud, *J. Phys.: Conf. Ser.* **126**, 012055 (2008).
- <sup>9</sup>A. Thiaville and J. Miltat, *J. Appl. Phys.* **68**, 2883 (1990).
- <sup>10</sup>A. Thiaville, J. H. Ben Youssef, Y. Nakatani, and J. Miltat, *J. Appl. Phys.* **69**, 6090 (1991).
- <sup>11</sup>A. Thiaville, J. Miltat, and J. Ben Youssef, *Eur. Phys. J. B* **23**, 37 (2001).
- <sup>12</sup>A. Hubert, *AIP Conf. Proc.* **18**, 178 (1974).
- <sup>13</sup>J. C. Slonczewski, *AIP Conf. Proc.* **24**, 613 (1975).
- <sup>14</sup>Y. Nakatani and N. Hayashi, *IEEE Trans. Magn.* **24**, 3039 (1988).
- <sup>15</sup>J. Miltat, A. Thiaville, and P. Trouilloud, *J. Magn. Magn. Mater.* **82**, 297 (1989).
- <sup>16</sup>A. Masseboeuf, C. Gatel, J. C. Toussaint, A. Marty, and P. Bayle-Guillemaud, *Ultramicroscopy* **110**, 20 (2009).
- <sup>17</sup>G. Beutier, A. Marty, K. Chesnel, M. Belakhovsky, J. Toussaint, B. Gilles, G. Van der Laan, S. Collins, and E. Dudzik, *Physica B* **345**, 143 (2004).
- <sup>18</sup>S. Khizroev and D. Litvinov, *Perpendicular Magnetic Recording* (Kluwer Academic, Boston, 2004).
- <sup>19</sup>J. Dooley and M. De Graef, *Micron* **28**, 371 (1997).
- <sup>20</sup>J. Chapman, *J. Phys. D* **17**, 623 (1984).
- <sup>21</sup>D. Paganin and K. Nugent, *Phys. Rev. Lett.* **80**, 2586 (1998).
- <sup>22</sup>Y. Aharonov and D. Bohm, *Phys. Rev.* **115**, 485 (1959).
- <sup>23</sup>A. Hubert and R. Schäfer, *Magnetic Domains* (Springer, Berlin, 1998).
- <sup>24</sup>T. Jourdan, A. Marty, and F. Lançon, *Phys. Rev. B* **77**, 224428 (2008).
- <sup>25</sup>T. Jourdan, A. Masseboeuf, F. Lançon, P. Bayle-Guillemaud, and A. Marty, *J. Appl. Phys.* **106**, 073913 (2009).
- <sup>26</sup>T. Jourdan, “Multiscale approach for magnetism. Application to structural heterogeneities and magnetic singularities,” Ph.D. thesis, Université Joseph Fourier—Grenoble, 2008.
- <sup>27</sup>V. Gehanno, A. Marty, B. Gilles, and Y. Samson, *Phys. Rev. B* **55**, 12552 (1997).
- <sup>28</sup>A. Hubert, *J. Magn. Magn. Mater.* **2**, 25 (1976).
- <sup>29</sup>A. Masseboeuf, F. Cheynis, J. C. Toussaint, O. Fruchart, C. Gatel, A. Marty, and P. Bayle-Guillemaud, *Mater. Res. Soc. Symp. Proc.* **1026**, 1026-C22 (2007).